Springer

KSME

Journal of Mechanical Science and Technology 33 (6) (2019) 2929~2940
www.springerlink.com/content/1738-494x(Print)/1976-3824(Online)
DOI 10.1007/s12206-019-0540-6

Lane departure avoidance by man-machine cooperative control based on EPS and ESP systems †

Xuanyao Wang[1,2,3,*] and Yi Cheng[1]

[1]*School of Mechanical Engineering, Anhui University of Science and Technology, Huainan, China*
[2]*Anhui Key Laboratory of Mine Intelligent Equipment and Technology, Anhui University of Science and Technology, Huainan, China*
[3]*State Key Laboratory of Mining Response and Disaster Prevention and Control in Deep Coal Mines, Anhui University of Science and Technology, Huainan, China*

(Manuscript Received November 3, 2018; Revised January 31, 2019; Accepted March 4, 2019)

Abstract

The ability to avoid lane departure has become an important feature for development of driving assistance technology, and the design of lane departure avoidance system (LDAS) which can achieve cooperative control with human driver is still a challenge. This paper presented a new lane departure decision algorithm along with main parameters of the electric power steering (EPS) and electronic stability program (ESP) system's sensor. During normal situations, steering control based on EPS system was involved to avoid lane departure. However, when the vehicle reached the handling limits, both steering and braking control collaborated together to avoid lane departure based on EPS and ESP systems. Due to the time varying vehicle speed and the uncertainty of tire cornering stiffness, a gain scheduling brake controller was designed based on the energy-to-peak performance indicator, and an upper monitor was designed for activation the braking controller to ensure comfortable ride. Because the relationship between the lane departure degree with a lateral offset in the single-point preview and the driver torque could not be accurately described, a man-machine cooperative control fuzzy observer for the LDAS was designed. In order to accomplish smooth switching for driving mode to ensure ride comfort, a switching criterion was proposed. The proposed method was evaluated via numerical simulation by CarSim/Simulink. A hardware-in-the-loop test platform was set up, and the effectiveness of the proposed control strategy was compared via the driver-in-the-loop experiment. The obtained results show that the proposed man-machine cooperative control strategy not only can return the vehicle to the normal lane effectively, but also realize smooth switching from man-machine cooperative control to driver control.

Keywords: Lane departure; Fuzzy observer; Man-machine cooperative control; Smooth switching; EPS and ESP systems

1. Introduction

Driving assistance technology is an important part of intelligent vehicle development, although current autonomous driving technology is not yet capable of guaranteeing absolutely reliability. According to statistics published by Vaa [1], approximately 50 % of traffic accidents are caused by vehicles deviating from their normal driving lane. The main reasons for this include distractions while driving, inattention, or fatigue. Our purpose in studying driving assistance technology is to improve the safety of driving, especially through the development of active safety technology to avoid traffic accidents.

A lane departure warning system (LDWS) notifies the driver in the event that the vehicle is detected deviating from the lane without activating the turn signal. The notification may include a steering wheel vibration or other indication to remind the driver that the vehicle is deviating from the lane, thereby providing more reaction time to the driver and greatly reducing the number of accidents caused by lane departure. The assistance decision-making algorithm in the LDWS is based on the time to line crossing (TLC). If the threshold value of the TLC is too conservative, then it will lead to false alarms and seriously affect the mood of the driver [2, 3]. Descriptions of various lane departure recognition algorithms can be found in Refs. [4-6].

The lane departure assistance system (LDAS) is based on the LDWS. The most commonly used steering actuator in the LDAS is the motor, which is based on the electric power steering (EPS). Zhang and Bolia [7, 8] developed a lane keeping control that was based on the EPS and was able to solve coordination problems between the EPS components and the lane keeping execution algorithm. A wire control steering system consisting of actuators for the LDAS and lane keeping assistance system (LKAS) was proposed by Refs. [9-11], but the wire control steering system cost is too high. A differential

*Corresponding author. Tel.: +86 554 6668932, Fax.: +86 554 6668934
E-mail address: xuanyaowang@126.com
† Recommended by Associate Editor Sangyoon Lee

braking control, as described in Refs. [12-14], or a differential driving control that generates a yawing moment, are both able to correctly return the vehicle to the normal lane; however, differential braking affects the riding comfort, and differential driving is more suitable for the wheel motor. The LDAS was proposed by Lee [15] and was based on a steering and braking system, however, man-machine cooperative control was not considered. The man-machine cooperative control helps the driver simultaneously with his own correct actions on the steering wheel for vehicles equipped with a conventional steering column, and for existing LDAS any torque imposed on the steering wheel by the driver could be considered as a disturbance input. In order to improve vehicle active safety, the cooperative control is needed to reduce human-machine conflict, and assign the steering control either to the driver or to the assistance system by a switching strategy.

Man-machine cooperative control needs to allow input from the driver, while overlaying the steering torque generated by an actuator. The key to the LDAS is determining the proper weight distribution in the man-machine cooperative control system. The control strategy used in the LDAS was proposed by Enache [4] and is based on the theory of composite Lyapunov functions and linear matrix inequality switching, but the algorithm is complicated. A tactile guidance system that was able to realize shared steering control by both the driver and actuator was proposed by Mulder [16]. A model of a driver-vehicle-road closed lane keeping system was established by Saleh [17], and realized man-machine coordinated control of the LKAS based on preview control through a man-machine coordinated index. Man-machine coordination control was realized by Sentouh [18] and was based on a model of the driver that was able to identify inattention in order to minimize interventions by the LKAS controller. A designed man-machine cooperation controller for obstacle avoidance was proposed based on the T-S fuzzy theory [19]. The real-time online status of the driver was not considered in the methods mentioned above. The linear parameter varying (LPV)/H∞ steering angle controller and second-order sliding mode steering torque controller in the LDAS were designed by Tan [20] based on the man-machine weight allocation module. The characteristics of the driver were considered when designing the steering controller, but the nature of the man-machine weight allocation method was complicated. In order to coordinate the online LDAS switching smoothly from man-machine cooperative control to driver control, more research is needed to optimize the man-machine weight allocation when the driver is experiencing different conditions.

The main function of the EPS is to provide power assisted steering in order to reduce the burden on the driver, and improve their comfort. In addition, the EPS provides a good foundation for the further development of assisted driving. The steering angle and steering torque controller in the LDAS were designed based on the EPS, and the LDAS is an expansion of the EPS function. During normal situations, steering control based on EPS system was involved to avoid lane departure. However, under complex driving conditions when the vehicle reached the handling limits, both steering and braking collaborated together to avoid lane departure based on EPS and ESP system. Due to the time varying vehicle speed and the uncertainty of tire cornering stiffness, robust braking control is still a challenge.

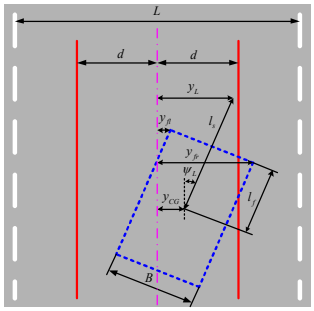

Fig. 1. Schematic diagram for vehicle in the lane.

In this paper, we study the man-machine cooperative control problem as well as the avoiding lane departure enhancement based on the EPS system and ESP system. The main contributions of this work can be summarized as follows: (1) In the man-machine cooperative control aspect, a fuzzy observer is designed based on the lateral offset of the single-point preview and the driver torque. A man-machine switching criterion is proposed which realizes smooth switching from man-machine cooperative control to driver control. (2) In the controller design aspect, during normal situations a LDAS controller is designed based on the steering system. A gain scheduling braking controller is designed based on the energy-to-peak performance indicators when the vehicle reached the handling limits. The coordination of steering and braking controllers is achieved through an upper monitor. (3) On the simulation side, the man-machine cooperative control is simulated by CarSim/Simulink, and a hardware-in-the-loop test platform is set up based on the EPS system and ESP system.

This paper is organized as follows. Sec. 2 describes the proposed lane departure decision algorithm. Sec. 3 provides the design procedures for the proposed steering angle and steering torque controllers, the proposed man-machine cooperative control fuzzy observer, the proposed gain scheduling braking controller, and the determining factors for switching from man-machine cooperative control mode to driver control mode. Sec. 4 compares the performance of the LDAS with the controller, and man-machine cooperative control mode based on CarSim/Simulink. Sec. 5 presents the LDAS hardware-in-the-loop test platform, which is based on the EPS/ESP systems and CarSim/LabVIEW RT. The results of the proposed strategy of the LDAS demonstrate its ability to correctly return the vehicle to the normal lane in man-machine cooperative control mode. Sec. 6 outlines our conclusions.

2. Lane departure decision algorithm

In order to avoid falsely activating the LDAS when the

driver is intentionally driving the vehicle near the lane border, a safe driving zone was defined by Enache [4], which meant that if vehicle was driving in the safe zone, then the LDAS would not intervene. The safe driving zone in the lane is shown in Fig. 1, where lf is the distance from the vehicle center of mass to the front axle, L is the lane width, ls is the single-point preview distance, y_L is the lateral offset, and the width of the safe central area is $2d$ where $2d < L$. A counterclockwise direction of deviation for the yaw angle is considered to be positive, the lateral offset of the single-point preview and the vehicle mass center is considered positive when it is in the center line on the left side of the road. Based on vehicle front wheel track B, the lateral offset of the front left and front right wheels of the vehicle can be determined based on the geometric relationships.

$$\begin{cases} y_{fl} = y_{CG} + l_f \sin\psi_L + \dfrac{B\cos\psi_L}{2} \\ y_{fr} = y_{CG} + l_f \sin\psi_L - \dfrac{B\cos\psi_L}{2} \end{cases}. \tag{1}$$

In general, if the deviation of the yaw angle ψ_L in Eq. (1) is very small, $\sin\psi_L \approx \psi_L$ and $\cos\psi_L \approx 1$. The lateral offset of the single-point preview and the deviation of the yaw angle are determined based on the CCD camera preview information via image processing algorithms. Therefore, the lateral offset of the vehicle mass center is $y_{CG} = y_L - l_s\psi_L$.

$$\begin{cases} y_{fl} = y_L + (l_f - l_s)\psi_L + \dfrac{B}{2} \\ y_{fr} = y_L + (l_f - l_s)\psi_L - \dfrac{B}{2} \end{cases}. \tag{2}$$

According to Eq. (2), whether the conditions of both front left and front right wheel on the vehicle are in the safe driving zone of the LDAS is determined by:

$$-(2d - B)/2 \le y_L + (l_f - l_s)\psi_L \le (2d - B)/2\,. \tag{3}$$

The on-center handling area is often referred to as the driving conditions in which the vehicle is in or around the neutral position, the steering wheel angle and lateral acceleration are both low, and the steering wheel angular rate is slow. Inattention or fatigue on the part of the driver may cause the vehicle to deviate from its lane. Based on the on-center handling characteristics, the decision condition for lane departure is:

$$\begin{aligned} &|T_d| < 2\ \text{N.m} \wedge\ d_{DLC}\ 0.4\ \text{m} \wedge\ |\delta_{sw}| < 20\ \text{deg} \\ &\wedge\ |\omega_{sw}| < 50\ \text{deg/s} \wedge\ |r| < 6\ \text{deg/s} \end{aligned} \tag{4}$$

where "∧" denotes the logical AND in Eq. (4). T_d is the driver torque, d_{DLC} is the distance to line crossing, δ_{sw} is the steering wheel angle, ω_{sw} is the steering wheel angular rate, and r is the yaw rate. Threshold constant of d_{DLC} can be found in Ref. [14], and threshold constants of T_d, δ_{sw}, ω_{sw} and r can be found in Refs. [17, 21], for lane keeping or normal or emergency lane changing, the conditions under which the driver receives the highest steering weight are:

$$\begin{aligned} &2\ \text{N.m} \le |T_d| < 6\ \text{N.m} \wedge \left|y_L + (l_f - l_s)\psi_L\right| < (2d - B)/2 \\ &\vee |T_d| \ge 6\ \text{N.m} \vee\ \text{Turn signal.} \end{aligned} \tag{5}$$

where "∨" denotes the logical OR in Eq. (5).

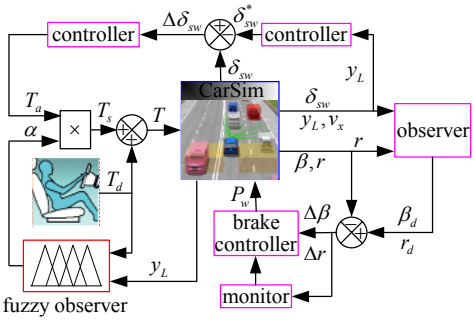

T_s : Actual steering torque of the LDAS controller
β : Side-slip angle
v_x : Vehicle longitudinal speed
P_w : Wheel cylinder pressure

Fig. 2. Block diagram of LDAS control based on the steering and braking systems.

3. LDAS control

To ensure that the LDAS is able to realize man-machine cooperative control operations under complicated driving conditions, we propose an LDAS control strategy based on steering and braking systems, which are both reliable electromechanical executive systems that have been widely used in passenger cars. This makes it easier to integrate them into existing systems. In order to ensure riding comfort when the difference between the expected and actual yaw rates is greater than the set threshold of 15 deg/s which was derived from tuning, and the brake controller based on the braking system is able to intervene through LDAS control. That is to say that the controller based on the steering system is prioritized to automatically activate the LDAS. The block diagram of the man-machine cooperative control algorithm based on the steering and braking systems is shown in Fig. 2. The control layer in the man-machine cooperative control mode of the LDAS is composed of the driver model, the steering angle and steering torque controller of the LDAS, and the fuzzy observer of the man-machine cooperative control coefficient.

3.1 LDAS controller design based on the steering system

The road information in the preview area of the LDAS is acquired by a visual sensor, such as a CCD camera, and the

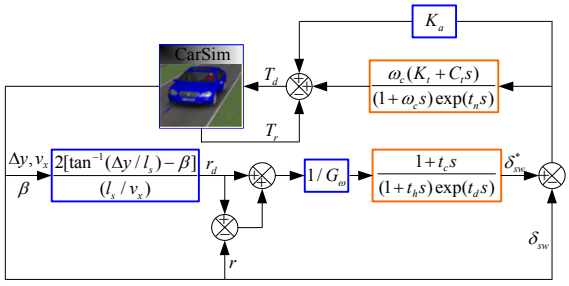

Fig. 3. Driver model.

single-point preview distance setting l_s = 15 m. The input to the path tracking upper controller of the LDAS is $\Delta y_L = 0 - y_L$, which is the difference between the expected and actual values of the single-point preview lateral offset, and the controller output is δ_{sw}^* that corresponds to the desired steering angle. In this case, the transfer function of the controller is:

$$\frac{\delta_{sw}^*}{\Delta y_L} = K_{p1} + K_{I1}\frac{1}{s} \tag{6}$$

The controller parameters are set to K_{P1} = 30 and K_{I1} = 0.01 in Eq. (6).

As shown in Fig. 2, the input to the path tracking lower LDAS controller is $\Delta\delta_{sw}$ which is the difference between the expected and actual values of the steering angle, and the output of the controller is T_a that corresponds to the desired steering torque. In this case, the transfer function of the controller is:

$$\frac{T_a}{\Delta\delta_{sw}} = K_{p2} + K_{d2}\frac{N_0}{1+N_0/s} \tag{7}$$

The controller parameters are set to K_{P2} = 12 and K_{d2} = 0.01 in Eq. (7), and the filter coefficient N_0 = 100. The desired motor torque is $T_m = T_a/N$, where the worm gear and worm gear reduction ratio is N. Finally, the steering torque closed loop control is realized by the output PWM signals of the lower proportional-integral-derivative (PID) controller that drive motor.

3.2 Driver model

The man-machine cooperative control mode was simulated by the LDAS controller using a lane keeping neuromuscular dynamics model based on the physiological and psychological characteristics of a driver. In order to avoid actual manipulation on the part of the driver from creating uncertainty that prevents the objective evaluation of the man-machine cooperative control performance, the driver model shown in Fig. 3 was adopted to simulate the man-machine cooperative control mode. The model is composed of an integrated-type steering angle input model based on a vehicle trajectory prediction and the neuromuscular system of the driver, where $\Delta y = -y_L/\cos\psi_L$. The parameters used for the driver model can be found in Ref. [22]. The single-point preview distance was set to l_s = 15 m and the preview time to $t_p = l_s/v_x$.

Table 1. Fuzzy rules of mutual control coefficient.

T_d	y_L				
	NB	NM	Z	PM	PB
NB	VL	M	Z	M	L
NM	VL	S	Z	S	L
Z	VL	S	S	S	VL
PM	L	S	Z	S	VL
PB	L	M	Z	M	VL

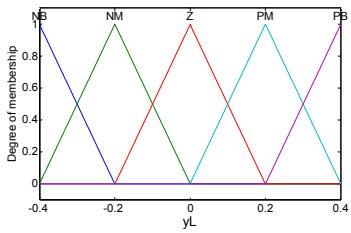

Fig. 4. Membership functions of y_L.

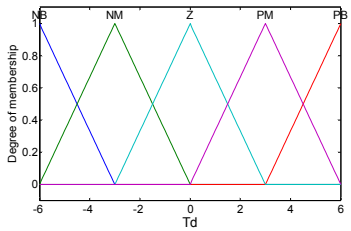

Fig. 5. Membership functions of T_d.

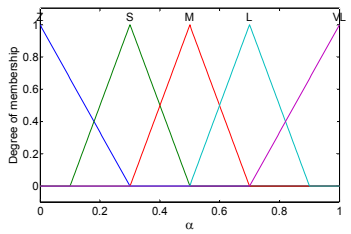

Fig. 6. Membership functions of α.

3.3 Man-machine cooperative control strategy

The relationship between the degree of lane departure, the lateral offset of the single-point preview based on the visual sensor (CCD camera), and the driver torque cannot be accurately described. In other words, the control process signal evaluation index cannot be quantitatively determined. Fuzzy control theory is an effective way to solve this problem. While in operation, the system constantly tests the lateral offset and driver torque based on the fuzzy control rules, and adjusts the man-machine mutual control coefficient α, which causes α to dynamically switch between 0 and 1. In this manner, the sys-

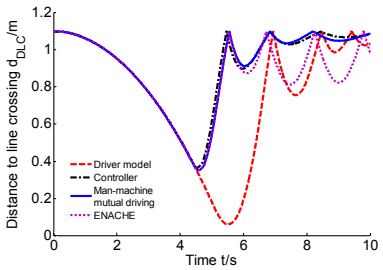

Fig. 7. Distance to line crossing.

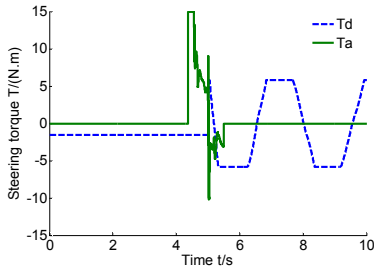

Fig. 8. Steering torque.

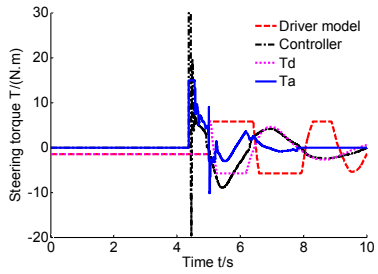

Fig. 9. Steering torque.

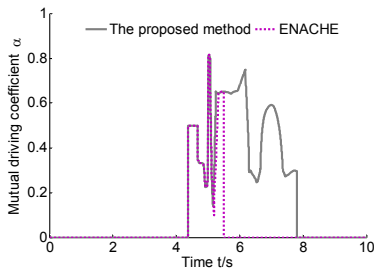

Fig. 10. Mutual control coefficient.

tem is able to switch from man-machine cooperative control mode to driver control mode (and vice versa).

As shown in Fig. 2, the inputs to the fuzzy observer are the lateral offset and driver torque, and the output from the fuzzy observer is the mutual control coefficient of the driver and LDAS controller. The fuzzy input membership functions are shown in Figs. 4 and 5, and the fuzzy output membership functions are shown in Fig. 6. The basic domain of discourse of the lateral offset is [-0.4, 0.4] m, the basic domain of discourse of the driver torque is [-6, 6] N.m, and the basic domain of discourse of the mutual control coefficient is [0, 1]. The fuzzy subset of the lateral offset and driver torque is {NB, NM, Z, PM, PB}, the fuzzy subset of the output of the fuzzy observer (mutual control coefficient) is {Z, S, M, L, VL}, and the fuzzy rule table of the mutual control coefficient is shown in Table 1.

3.4 Switching strategy

One of the key problems in the LDAS is how implement the switch from man-machine cooperative control mode to driver control mode when the system is not in steady state. It is possible to transiently satisfy the conditions in Eq. (5) if all of the steering control weight is assigned to the driver. However, the vehicle may not be able to accomplish a smooth switch to driver control; therefore, a judge index τ_α is proposed, which means that the duration is below the threshold value α_{th} of the man-machine cooperative control coefficient, where $\alpha_{th} = 0.35$. The conditions under which the LDAS switches to driver control mode are:

$$\tau_\alpha \geq 0.5\ \text{s} \vee |T_d| \geq 6\text{N.m} \vee \text{Turn signal}. \tag{8}$$

The CarSim/Simulink simulation parameters are as follows. The tire-road friction coefficient is 0.85, the lane width is 3.75 m, the speed is 120 km/h, and the road model consists of a 1 km straight road. The output torque of the steering controller is limited to 15 N.m. Driver fatigue or inattention is simulated by a 1 N.M constant clockwise steering torque. In the proposed lane departure decision algorithm, the steering controller is activated at 4.37 s. When the driver characteristics are considered, it is not likely that the driver and steering controller participate at the same time in correcting the vehicle back to the normal lane. Consequently, the driver model is set to a concentration of driving state of 5 s, and the output torque of the driver model is limited to 5.8 N.m. The man-machine switching principle proposed in Ref. [4] is represented by "Enache" in the figure. The d_{DLC} is shown in Fig. 7, although the driver model, steering controller, and man-machine cooperative control mode in the LDAS with different switching criteria can correctly return the vehicle to its normal lane. The minimum distance to line crossing is 0.06 m under the driver model control, while the minimum distance to line crossing under the remaining three control methods is approximately 0.35 m. Therefore, the ability of the latter three methods to correct the vehicle back to the normal lane is better than that for the driver control mode. The steering torque, as shown in Fig. 8, is based on the man-machine switching principle of "Enache" and meets the switch principle at 5.55 s. At this time, the whole steering control weight is given to the driver; however, it is apparent that the driver is not able to smoothly assume control of the vehicle. The steering torque in the man-machine switching principle proposed in this paper is shown in Fig. 9, the man-machine mutual control coefficient is shown in Fig. 10, the steering controller of LDAS stops running at 7.82 s, the vehicle smoothly switches to driver control, and the effectiveness of the proposed man-machine switch control strategy has been verified.

3.5 Braking controller

The brake controller in the LDAS was designed based on the linear two degrees of freedom vehicle model. The system state equation can be expressed as:

$$\dot{\boldsymbol{x}}(t) = \boldsymbol{A}\boldsymbol{x}(t) + \boldsymbol{B}_1 u_1(t) + \boldsymbol{B}_2 u(t) . \tag{9}$$

The state vector in Eq. (10) is $\boldsymbol{x} = [\beta, r]^T$, $u_1 = \delta_f$, $u(t) = \Delta M_z$,

$$\boldsymbol{A} = \begin{bmatrix} -\dfrac{C_f + C_r}{m v_x} & -1 + \dfrac{l_r C_r - l_f C_f}{m v_x^2} \\ \dfrac{l_r C_r - l_f C_f}{I_z} & -\dfrac{l_f^2 C_f + l_r^2 C_r}{I_z v_x} \end{bmatrix},$$

$$\boldsymbol{B}_1 = \begin{bmatrix} \dfrac{C_f}{m v_x} \\ \dfrac{l_f C_f}{I_z} \end{bmatrix}, \quad \boldsymbol{B}_2 = \begin{bmatrix} 0 \\ \dfrac{1}{I_z} \end{bmatrix}.$$

where the front wheel steering angle is δ_f, the correct yaw moment is ΔM_z, the front and rear tire cornering stiffness is C_f and C_r, respectively, the vehicle mass is m, and the yaw moment of inertia is I_z. If the desired values of β_d and r_d are used as the state variables in Eq. (9), when the system desired input is δ_f, and the linear two degree of freedom vehicle handling characteristic state equation can be expressed as:

$$\dot{\boldsymbol{x}}_d(t) = \boldsymbol{A}_d \boldsymbol{x}_d(t) + \boldsymbol{B}_d \delta_f . \tag{10}$$

In Eq. (10), $\boldsymbol{x}_d = [\beta_d, r_d]^T$, setting $\boldsymbol{e}(t) = \boldsymbol{x}(t) - \boldsymbol{x}_d(t)$, according to Ref. [22], the system state equation is:

$$\dot{\boldsymbol{e}}(t) = \boldsymbol{A}\boldsymbol{e}(t) + \boldsymbol{B}_1 \Delta\delta_f + \boldsymbol{B}_2 u(t) . \tag{11}$$

The desired side-slip angle β_d of the LDAS can be found in Ref. [23], and the desired yaw rate r_d of the LDAS can be found in Ref. [24].

The tire cornering stiffness is one of the important parameters in a vehicle dynamics control system, due to the fact that the tire cornering stiffness is influenced by various factors, such as the vehicle weight, road adhesion coefficient, tire pressure, etc., which is to say that the tire cornering stiffness is not a fixed value. The tire cornering stiffness with uncertainty can be represented as:

$$\begin{cases} C_f = C_{f0} + \Delta C_f N(t) \\ C_r = C_{r0} + \Delta C_r N(t) \end{cases}, \ |N(t)| \le 1 .$$

where C_{f0} and C_{r0} are the front and rear tire nominal cornering stiffness, respectively; C_f and C_r are the front and rear tire actual cornering stiffness, respectively; and ΔC_f and ΔC_f are the amplitude of the front and rear tire cornering stiffness, respectively.

In order to improve the ability of LDAS correct vehicle return to normal lane, need to make $\Delta\beta$ as small as possible, the yaw rate r as possible tracking desired yaw rate rd, that is to say Δr as small as possible, so choose two control output as follows,

$$\begin{cases} z_1(t) = \boldsymbol{C}_1 \boldsymbol{e}(t) \\ z_2(t) = \boldsymbol{C}_2 \boldsymbol{e}(t) \end{cases} . \tag{12}$$

In Eq. (12), $C_1 = [1\ 0]$, $C_2 = [0\ 1]$.

In Eq. (12), $\Delta\delta_f$ is the external disturbance input to the system dynamics Eq. (11). In order to prevent the influence of an external disturbance on the controlled output, the energy-to-peak performance is chosen as follows:

$$\begin{cases} \|z_1\|_\infty = \gamma_1 \|\Delta\delta_f\|_2 \\ \|z_2\|_\infty = \gamma_2 \|\Delta\delta_f\|_2 \end{cases} . \tag{13}$$

Based on the rear wheel braking scheme, the state feedback controller for the gain scheduling of the LDAS is:

$$\Delta M_z(t) = \boldsymbol{K}(\xi)\boldsymbol{e}(t) . \tag{14}$$

In Eq. (14), $\boldsymbol{K}(\xi)$ is state feedback gain, $\xi = [\xi_1, \xi_2]^T$.

Based on the brake controller, the closed-loop system of the state space model of the LDAS is:

$$\dot{\boldsymbol{e}}(t) = (\boldsymbol{A}(\xi) + \Delta\boldsymbol{A}(\xi) + \boldsymbol{B}_2\boldsymbol{K}(\xi))\boldsymbol{e}(t) + (\boldsymbol{B}_1(\xi) + \Delta\boldsymbol{B}_1(\xi))\Delta\delta_f .$$

Corollary 1 Given a disk region $\boldsymbol{D}$ (q, r), if there exist a positive-definite matrices $\boldsymbol{Y} = \boldsymbol{Y}^T$, matrices $\hat{\boldsymbol{K}}_i$, and scalars $\varepsilon_{1,i}$, $\varepsilon_{2,i}$ and $\varepsilon_{3,i}$, the minimum energy-to-peak performance index γ_1, when other energy-to-peak performance index is constrained into a prescribed level γ_2 can be obtained by solving the following minimization problem [25],

$$\begin{aligned} &\min \gamma_1^2 I \\ &\text{s.t.} \begin{bmatrix} -\gamma_1^2 \boldsymbol{I} & \boldsymbol{C}_1 \\ * & -\boldsymbol{Y} \end{bmatrix} < 0 \\ &\begin{bmatrix} -\gamma_2^2 \boldsymbol{I} & \boldsymbol{C}_2 \\ * & -\boldsymbol{Y} \end{bmatrix} < 0 \\ &\Theta_{ij} + \Theta_{ji} < 0 \\ &\Xi_{ij} + \Xi_{ji} < 0 . \end{aligned} \tag{15}$$

In Eq. (15), where

$$\Theta_{ij} = \begin{bmatrix} \hat{\boldsymbol{\Omega}}_1 & \boldsymbol{B}_{1,i} & \varepsilon_{1,i}\boldsymbol{E}_{1,j} & \varepsilon_{2,i}\boldsymbol{E}_{2,j} & (\boldsymbol{F}_{1,i}\boldsymbol{Y})^T & 0 \\ * & -\boldsymbol{I} & 0 & 0 & 0 & \boldsymbol{F}_{2,i}^T \\ * & * & -\varepsilon_{1,i}\boldsymbol{I} & 0 & 0 & 0 \\ * & * & * & -\varepsilon_{2,i}\boldsymbol{I} & 0 & 0 \\ * & * & * & * & -\varepsilon_{1,i}\boldsymbol{I} & 0 \\ * & * & * & * & * & -\varepsilon_{2,i}\boldsymbol{I} \end{bmatrix}$$

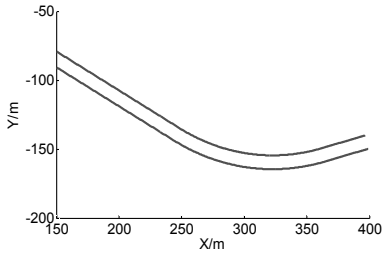

Fig. 11. Tracking path.

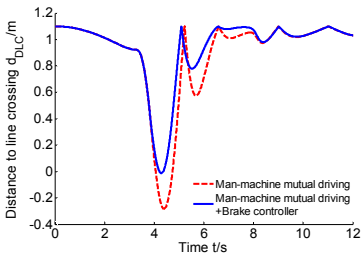

Fig. 12. Distance to line crossing.

$$\Xi_{ij}=\begin{bmatrix} -r\boldsymbol{Y} & q\boldsymbol{Y}+\boldsymbol{A}_i\boldsymbol{Y}+\boldsymbol{B}_2\hat{\boldsymbol{K}}_i & \varepsilon_{3,i}\boldsymbol{E}_{1,j} & 0 \\ * & -r\boldsymbol{Y} & 0 & (\boldsymbol{F}_{1,i}\boldsymbol{Y})^T \\ * & * & -\varepsilon_{3,i}\boldsymbol{I} & 0 \\ * & * & * & -\varepsilon_{3,i}\boldsymbol{I} \end{bmatrix}$$

where $\hat{\boldsymbol{\Omega}}_1=(\boldsymbol{A}_i\boldsymbol{Y}+\boldsymbol{B}_2\hat{\boldsymbol{K}}_i)+(\boldsymbol{A}_i\boldsymbol{Y}+\boldsymbol{B}_2\hat{\boldsymbol{K}}_i)^T$, $1\le i\le j\le 2$.

The feedback gains can be calculated by:

$$\boldsymbol{K}_i=\hat{\boldsymbol{K}}_i\boldsymbol{Y}^{-1}. \tag{16}$$

The state feedback gain of the optimal energy-to-peak stabilization controller can be calculated as:

$$\boldsymbol{K}(\xi)=\xi_1\boldsymbol{K}_1+\xi_2\boldsymbol{K}_2. \tag{17}$$

The vehicle model that was used is an E-Class/Sedan in the CarSim software, which sets the range of the vehicle speed $v_x \in [20,40]$. The controller gains were acquired by the LMI toolbox in MATLAB.

4. Simulation based on CarSim/Simulink

An E-Class/Sedan was used as the simulation vehicle model in CarSim. The tire-road friction coefficient was 0.85, the vehicle speed was 90 km/h, the road model was Alt3 from the Federal Highway Administration (FHWA), the tracking path is shown in Fig. 11, the lane width was 3.75 m, and the simulation time was 12 s. The brake system was simple, and the relationship between the wheel brake torque and the pressure of the wheel cylinder was 150 N.m/MPa. The largest brake wheel cylinder pressure was 12 MPa for a saturated sector. The maximum assistive torque applied by the steering controller was 30 N.m. The errors due to driver inattention or fatigue

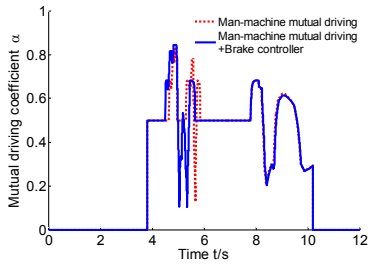

Fig. 13. Mutual control coefficient.

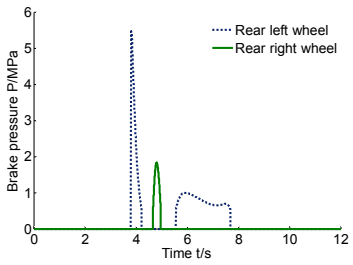

Fig. 14. Brake pressure.

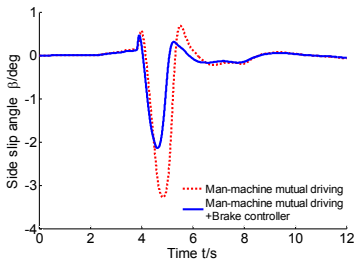

Fig. 15. Side slip angle.

were simulated by the driver model and the man-machine cooperative control mode at 3.8 s through the proposed lane departure criteria. The distance to line crossing is shown in Fig. 12, the man-machine cooperative control coefficient is shown in Fig. 13, the LDAS stopped at 10.2 s, and the EPS and ESP systems restored the LDAS to the normal working mode.

Due to the high vehicle speed, the small curvature radius of the corner, and the lack of predictability in the proposed lane departure criteria, the vehicle may have already deviated from the normal lane in man-machine cooperative control mode. As shown in Fig. 12, the minimum distance to line crossing in the man-machine cooperative control mode was -0.28 m, while the minimum distance to line crossing in man-machine cooperative control and brake control mode was 0.01 m. If the brake controller was activated, it was able to address poor driving conditions and correctly return the vehicle to its normal lane.

The wheel cylinder pressure in the left and right wheels are shown in Fig. 14, and the maximum braking pressure was 5.5 MPa. The side-slip angle is shown in Fig. 15, the maximum side-slip angle in man-machine cooperative control mode was 3.3 deg, and the maximum side-slip angle of the man-machine cooperative control + brake controller mode was 2.1 deg. The

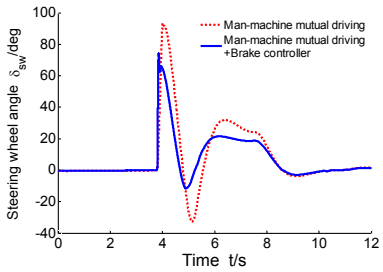

Fig. 16. Steering wheel angle.

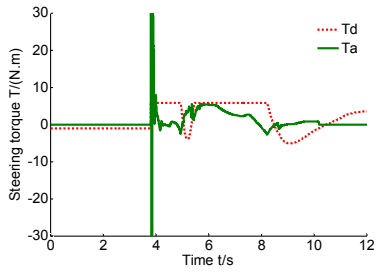

Fig. 17. Steering torque.

steering wheel angle is shown in Fig. 16, the maximum steering wheel angle of the man-machine cooperative control mode was 93.6 deg., and the maximum steering wheel angle of the man-machine cooperative control + brake controller mode was 74.2 deg. The driver model torque and assistant torque of steering controller is shown in Fig. 17 with the man-machine cooperative control + brake controller.

5. Hardware-in-the-loop simulation

In order to perform the hardware-in-the-loop test for the LDAS, a new controller was developed based on an EPS system to replace the original controller, and an actuator for the hydraulic pressure regulator was designed based on an ESP system. The LDAS hardware-in-the-loop test bench is shown in Fig. 18, and the signal flow diagram for the system is shown in Fig. 19. The hydraulic pressure regulator is the most important actuator in the electronic stability control system, and the fact that there are four independent tubes connected to the four-wheel cylinder means that the system can provide independent control of all four wheels, in a so-called four channel structure. The LDAS was designed based on a rear wheel brake control system; therefore, the hydraulic pressure regulator only needs to control the brakes for two wheels. The brake pressure readings from the wheel cylinder pressure sensors were sent through the wiring board to the data acquisition card.

The hardware-in-the-loop simulation conditions are the same as above and are based on the CarSim/LabVIEW RT. The scenario wherein a driver drifts outside of the normal lane due to fatigue or inattention and does not apply sufficient steering torque to recover within 2.2 s was simulated by the driver model. The road preview information lane departure decision algorithm detected the deviation of the vehicle from

Fig. 18. The test bench.

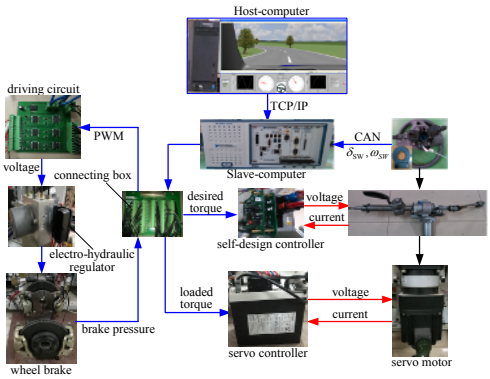

Fig. 19. Control signal flow diagram.

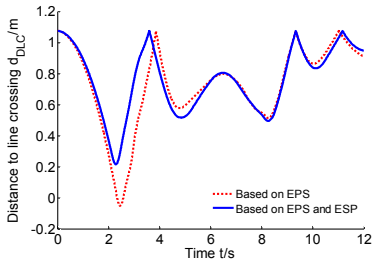

Fig. 20. Distance to line crossing.

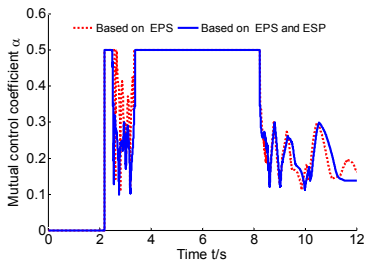

Fig. 21. The cooperative control coefficient.

the normal lane at 2.2 s. The driver and LDAS controller correctly returned the vehicle to its normal lane at the same time. In order to avoid the uncertainty caused by having an actual driver manipulate the system, a method for the objective evaluation of the man-machine cooperative control performance was constructed based on LabVIEW to build a driver model for correctly returning the vehicle to its normal lane. In

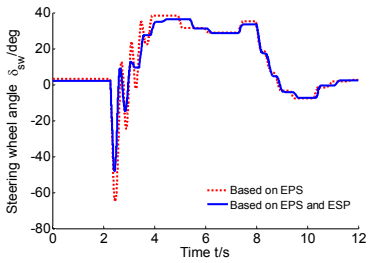

Fig. 22. Steering wheel angle.

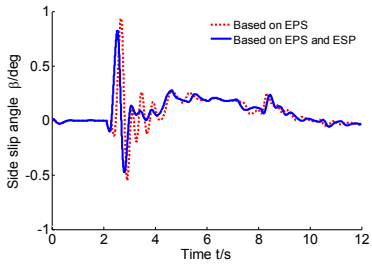

Fig. 25. Side slip angle.

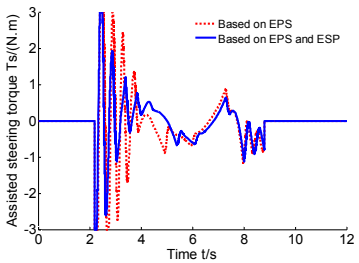

Fig. 23. Assisted steering torque of the controller.

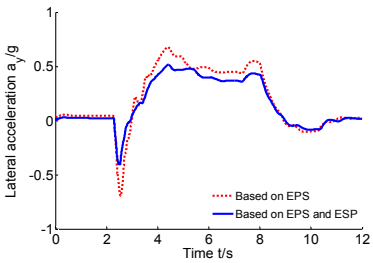

Fig. 26. Lateral acceleration.

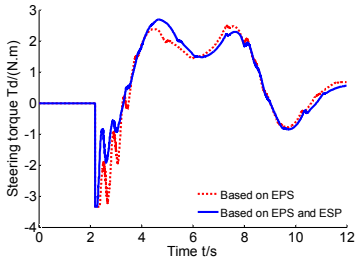

Fig. 24. Steering torque of the driver model.

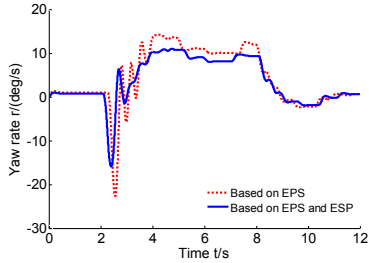

Fig. 27. Yaw rate.

order to simplify the expression in the figure, the LDAS man-machine cooperative control mode based on the EPS is denoted “based on EPS” in the figure, and the LDAS man-machine cooperative control based on the EPS and ESP systems is denoted “based on EPS and ESP” in the figure. The distance to line crossing is shown in Fig. 20, the minimum distance to line crossing of the former was -0.05 m and the front wheel of the vehicle had deviated from the normal lane, but the minimum distance to line crossing of the latter was 0.22 m, and the man-machine cooperative control coefficient is shown in Fig. 21. The proposed rule for switching between the man-machine cooperative control mode and completely giving the steering control to the driver occurs at 8.8 s. At this time, the EPS and ESP systems return to normal operation.

As shown in Fig. 20, the proposed man-machine cooperative control mode smoothly switches to driver independent control mode, and the LDAS with man-machine cooperative control not only correctly returns the vehicle to its normal lane, but also allows the vehicle to turn the corner. The steering wheel angle is shown in Fig. 22, the absolute maximum value of the steering angle of the former was up to 65 deg, the absolute maximum value of the steering angle of the latter was 48 deg, and the former steering angle was significantly jittery, which seriously affected the riding comfort. The steering torque of LDAS controller and the driver steering torque are shown in Figs. 23 and 24, respectively.

The side-slip angle is shown in Fig. 25, the maximum absolute value of the side-slip angle of the former was 2.3 deg, and the maximum absolute value of the side-slip angle of the latter was 1.6 deg. The lateral acceleration is shown in Fig. 26, the maximum absolute value of the lateral acceleration of the former was 0.7 g, and the maximum absolute value of lateral acceleration of the latter was 0.52 g. The yaw rate is shown in Fig. 27, the maximum absolute value of yaw rate of the former was 23 deg/s, and the maximum absolute value of yaw rate of the latter was 16 deg/s. The brake pressure of the rear left and rear right wheels is shown in Figs. 28 and 29, respectively, and the maximum braking pressure was 5 MPa. In conclusion, our results show that the proposed man-machine cooperative control strategy of the LDAS based on the EPS and ESP systems is able to correctly return the vehicle to its normal lane and can smoothly switch from man-machine cooperative control mode to driver control mode, and lane departures due to driver fatigue or inattention can be avoided.

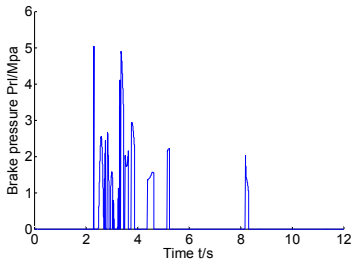

Fig. 28. Brake pressure of rear left wheel.

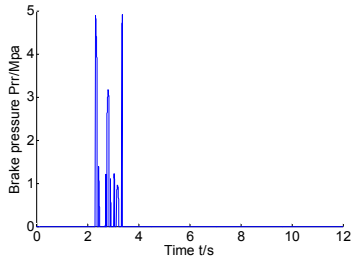

Fig. 29. Brake pressure of rear right wheel.

6. Conclusions

The steering angle controller of the LDAS was designed based on the lateral offset of the single-point preview steering angle. The steering torque controller of the LDAS was designed based on the difference between the desired steering angle and the practical steering angle, and the controller parameters were tuned. A lane departure decision algorithm was proposed that takes into account the LDAS safety zone based on the vision sensor preview information. In order for the LDAS to correctly return the vehicle to its normal lane under complex conditions, while considering the time-varying vehicle speed and uncertainty of the tire cornering stiffness, based on the energy-to-peak performance index a gain scheduling brake controller was designed. In order to ensure riding comfort, an upper monitor was designed for the brake controller.

A man-machine cooperative control fuzzy observer of LDAS was designed based on the theory of fuzzy control, and the fuzzy rules were determined. CarSim/Simulink was used to simulate the conditions under which a driver experiencing fatigue or inattention did not notice that the vehicle was deviating from the lane. In the simulation, the performance of the LDAS was compared with the driver model, the controller, and man-machine cooperative control. The results show that the proposed man-machine cooperative control strategy of the LDAS can correctly return the vehicle to its normal lane in a timely fashion, and can realize smooth switching from man-machine cooperative control mode to driver control mode.

A hardware-in-the-loop test platform for the LDAS was configured based on the EPS and ESP systems, and based on CarSim/LabVIEW RT the ability to correctly return the vehicle to the normal lane under complicated driving conditions was compared, and the results show that the LDAS based on the EPS and ESP systems is able to correctly return the vehicle to its normal lane and can smoothly switch from man-machine cooperative control mode to driver control mode, and lane departures due to driver fatigue or inattention can be avoided. The LDAS described in this article is designed to operate under high speed working conditions; however, our team did not to test the system under real-world high-speed driving conditions. For this reason, an important area of future work is for us to set up an experimental platform that includes a real vehicle and lane departure recognition system based on vision sensors in order to fully evaluate the performance of the proposed LDAS and man-machine cooperative control modes.

Acknowledgments

This work was supported by National Natural Science Foundation of China (Grant No. 51405004, 61471004), major science and technology projects in Anhui province (Grant No. 17030901060), Key research and development projects in Anhui province (Grant No. 1804a09020016) and Anhui Provincial Natural Science Foundation (Grant No. 1908085 ME159).

Nomenclature

L	: Lane width (m)
ls	: Single-point preview distance (m)
y_L	: Lateral offset (m)
d	: Width of the safe central area (m)
B	: Front wheel track (m)
ψ_L	: Yaw angle
y_{CG}	: Lateral offset of the vehicle mass center (m)
T_d	: Driver torque (N.m)
d_{DLC}	: Distance to line crossing (m)
δ_{sw}	: Steering wheel angle (º)
ω_{sw}	: Steering wheel angular rate (rad/s)
r	: Yaw rate (rad/s)
T_S	: Actual steering torque (N.m)
β	: Side-slip angle (º)
v_x	: Vehicle longitudinal speed (km/h)
P_w	: Wheel cylinder pressure (Mpa)
K_P	: Controller parameter
K_I	: Controller parameter
T_a	: Desired steering torque (N.m)
N_0	: Filter coefficient
T_m	: Desired motor torque (N.m)
N	: Worm gear reduction ratio
t_p	: Preview time (s)
α	: Man-machine mutual control coefficient
τ_α	: Judge index
α_{th}	: Threshold value
δ_f	: Front wheel steering angle (º)

ΔM_z : Correct yaw moment (N.m)
C_f : Front tire cornering stiffness (N/rad)
C_r : Rear tire cornering stiffness (N/rad)
m : Vehicle mass (kg)
I_z : Yaw moment of inertia (kg.m^2)
C_{f0} : Front tire nominal cornering stiffness (N/rad)
C_{r0} : Rear tire nominal cornering stiffness (N/rad)
$K(\xi)$: State feedback gain

References

[1] T. Vaa, M. Penttinen and I. Spyropoulou, Intelligent transport systems and effects on road traffic accidents: State of the art, *IET Intelligent Transport Systems*, 1 (2) (2007) 81-88.

[2] S. Mammar, S. Glaser and M. Netto, Time to line crossing for lane departure avoidance: A theoretical study and an experimental setting, *IEEE Transactions on Intelligent Transportation Systems*, 7 (2) (2006) 226-241.

[3] Y. Zhou, R. Xu, X. F. Hu and Q. T. Ye, A lane departure warning system based on virtual lane boundary, *Journal of Information Science & Engineering*, 24 (1) (2008) 293-305.

[4] N. M. Enache, S. Mammar, M. Netto and B. Lusetti, Driver steering assistance for lane-departure avoidance based on hybrid automata and composite Lyapunov function, *IEEE Transactions on Intelligent Transportation Systems*, 11 (1) (2010) 28-39.

[5] T. Hong, J. Kwon, K. Park, K. Lee, T. Hwang and T. Chung, Development of a driver's intention determining algorithm for a steering system based collision avoidance system, *SAE Technical Paper*, No. 2013-01-0054.

[6] A. Benine-Neto, S. Scalzi, S. Mammar, M. Netto and B. Lusetti, Model reference-based vehicle lateral control for lane departure avoidance, *International Journal of Vehicle Autonomous Systems*, 12 (3) (2014) 284-306.

[7] H. L. Zhang, Y. G. Luo, Q. Y. Jiang and K. Q. Li, Lane keeping system based on electric power steering system, *Automotive Engineering*, 35 (6) (2013) 526-531.

[8] P. Bolia, T. Weiskircher and S. Müller, Driver steering model for closed-loop steering function analysis, *Vehicle System Dynamics*, 52 (sup1) (2014) 16-30.

[9] E. J. Rossetter and J. C. Gerdes, Lyapunov based performance guarantees for the potential field lane-keeping assistance system, *Journal of Dynamic Systems, Measurement, and Control*, 128 (3) (2006) 510-522.

[10] D. Katzourakis, M. Alirezaei, J. C. de Winter, M. Corno, R. Happee, A. Ghaffari and R. Kazemi, Shared control for road departure prevention, *2011 IEEE International Conference on Systems, Man, and Cybernetics (SMC)*, USA (2011) 1037-1043.

[11] M. Doumiati, O. Sename, L. Dugard, J. J. Martinez-Molina, P. Gaspar and Z. Szabo, Integrated vehicle dynamics control via coordination of active front steering and rear braking, *European Journal of Control*, 19 (2) (2013) 121-143.

[12] T. Pilutti, G. Ulsoy and D. Hrovat, Vehicle steering intervention through differential braking, *Proceedings of 1995 American Control Conference-ACC'95*, Seatle, WA, USA, 3 (1995) 1667-1671.

[13] Z. Huang, Y. Wu, J. Liu and S. Hu, Research on lane departure avoidance system of high-speed vehicle, *Journal of Mechanical Engineering*, 49 (22) (2013) 157-163.

[14] J. Lee, J. Choi, K. Yi, M. Shin and B. Ko, Lane-keeping assistance control algorithm using differential braking to prevent unintended lane departures, *Control Engineering Practice*, 23 (2014) 1-13.

[15] J. Lee and K. Yi, Development of a coordinated strategy of steering torque overlay and differential braking for unintended lane departure avoidance, *SAE Technical Paper*, No. 2012-01-0281.

[16] M. Mulder, D. A. Abbink and E. R. Boer, The effect of haptic guidance on curve negotiation behavior of young, experienced drivers, *IEEE International Conference on Systems, Man and Cybernetics (SMC)*, Singapore (2008) 804-809.

[17] L. Saleh, P. Chevrel, F. Claveau, J. F. Lafay and F. Mars, Shared steering control between a driver and an automation: Stability in the presence of driver behavior uncertainty, *IEEE Transactions on Intelligent Transportation Systems*, 14 (2) (2013) 974-983.

[18] C. Sentouh, S. Debernard, J. C. Popieul and F. Vanderhaegen, Toward a shared lateral control between driver and steering assist controller, *IFAC Proceedings Volumes*, France (2010) 404-409.

[19] B. Soualmi, C. Sentouh, J. C. Popieul and S. Debernard, Automation-driver cooperative driving in presence of undetected obstacles, *Control Engineering Practice*, 24 (2014) 106-119.

[20] D. Tan, W. Chen, J. Wang, H. Wang and H. Huang, Human-machine sharing and hierarchical control based lane departure assistance system, *Journal of Mechanical Engineering*, 51 (22) (2015) 98-110.

[21] X. Wang, Q. Wang, Z. Gao and J. Wang, GC coordinated control strategy for lane departure avoidance system based on driver's lane change intention recognition, *Automotive Engineering*, 38 (7) (2016) 848-856.

[22] W. Chen, D. Tan, H. Wang, J. Wang and G. Xia, A class of driver directional control model based on trajectory prediction, *Journal of Mechanical Engineering*, 52 (14) (2016) 89-97.

[23] X. Yang, Z. Wang and W. Peng, Coordinated control of AFS and DYC for vehicle handling and stability based on optimal guaranteed cost theory, *Vehicle System Dynamics*, 47 (1) (2009) 57-79.

[24] P. Raksincharoensak, M. Nagai and M. Shino, Lane keeping control strategy with direct yaw moment control input by considering dynamics of electric vehicle, *Vehicle System Dynamics*, 44 (sup1) (2006) 192-201.

[25] H. Zhang, X. Zhang and J. Wang, Robust gain-scheduling energy-to-peak control of vehicle lateral dynamics stabilization, *Vehicle System Dynamics*, 52 (3) (2014) 309-340.

Xuanyao Wang received the B.Eng. and M.Eng. in mechanical engineering from Anhui University of Science and Technology, Anhui, China, in 2003 and 2006, respectively and the Ph.D. in automotive engineering from Hefei University of Technology, Anhui, China, in 2017. He is currently an Associate Professor with the School of Mechanical Engineering, Anhui University of Science and Technology, Anhui, China. His research interests mainly focus on vehicle system dynamics and control, automotive active safety technology and advanced driving assistance technology. He has authored about 20 publications in journals and conference proceedings.

Yi Cheng received the M.Eng. in mechanical engineering from Anhui University of Science and Technology, Anhui, China, in 2017. He is currently a master degree candidate at the School of Mechanical Engineering, Anhui University of Science and Technology, Anhui, China. His research interests mainly focus on automotive active safety technology and advanced driving assistance technology.